

# Shear Strength of GFRP RC Beams and Slabs

T. Alkhrdaji, M. Wideman, A. Belarbi, & A. Nanni

*Department of Civil Engineering, University of Missouri-Rolla, Missouri, USA*

**ABSTRACT:** ACI Committee 440 has proposed a new shear design approach for concrete members reinforced with fiber reinforced polymer (FRP) reinforcement that accounts for the amount and stiffness of FRP reinforcement. The applicability and limitations for the proposed design approach are not yet fully explored. In addition, the design approach imposes a very conservative strain limit for the FRP stirrups that may results in uneconomical use of the reinforcement. To investigate the proposed equations and their design limitations for shear, four beams reinforced with GFRP stirrups, three beams without stirrups, and six slabs that were designed to fail in shear were tested to failure as simply supported members. Test results indicated that the contribution of concrete to the internal shear resistance is influenced by the amount of the longitudinal reinforcement. The proposed formulae for predicting the shear resistance provided by concrete and GFRP stirrups were found to be overly conservative.

## 1 INTRODUCTION

Previous research indicated that FRP reinforced concrete (RC) flexural members designed for failure controlled by rupture of the FRP reinforcement (tension-controlled failure) have lower shear strength than steel RC members with equivalent flexural strength. To this effect, researches have proposed that design criteria for shear should account for the lower stiffness of the FRP reinforcement (Nagasaka et al. 1993, Sonobe et al. 1997, Michaluk et al. 1998).

In many cases, the design of FRP RC flexural member is governed by serviceability requirements, which results in flexural reinforcement amount beyond that needed to achieve the desired strength. For these members, the improved flexural behavior (e.g., strength and crack width) results in an improved internal shear resistance mechanism. This is also true for steel reinforced flexural sections where recent studied indicated that  $V_c$  is influenced by the ratio of flexural steel reinforcement and that for longitudinal steel reinforcement ratio  $\rho_s$  less than 0.012 the ACI equation of  $0.167\sqrt{f'_c}bd$  for  $V_c$  could be unconservative (ACI-ASCE Committee 426, 1978). Therefore, a shear design approach that does not considers the influence of both the stiffness and amount of longitudinal FRP reinforcement fails to account for the different contribution of internal shear resistance and can be, therefore, overly conservative.

ACI Committee 440 proposed a new shear design approach in its final draft that accounts for the amount and stiffness of longitudinal FRP reinforcement (ACI 440, 2000). However, the applicability and limitations for the proposed approach are not yet fully explored and it may not be equally applicable to beams and slabs. In addition, the design approach imposes a very conservative strain limit of 0.002 for the design of FRP stirrups that usually results in an uneconomical use of the reinforcement.

This paper presents the results of an experimental program aimed at producing additional data to examine the shear performance of RC members reinforced for shear and/or flexure using GFRP bars. GFRP bars are the most common type of FRP reinforcement due to their lower price, and have been used in a large number of projects worldwide and been therefore considered for this investigation.

### 1.1 Shear Strength of FRP Reinforced Members

For FRP RC flexural members without shear reinforcement, it was proposed that the internal shear resistance  $V_{c,f}$  is a function of the stiffness of longitudinal steel and FRP bars ( $E_s$  and  $E_f$ ) and can be evaluated as follows (Michaluk et al., 1998):

$$V_{c,f} = \frac{E_f}{E_s} V_c \quad (1)$$

The lower shear strength of FRP reinforced members could be related to a lower dowel resistance of FRP bars, smaller depth of compression block, and less effective aggregate interlock due to wider cracks. However, Eq. (1) is more appropriate for members lightly reinforced with FRP bars (tension-controlled failure). GFRP bars are commercially available with modulus  $E_f$  that is approximately 20% of the steel modulus. Therefore, when using GFRP bars, the shear strength of the member calculated with Eq. (1) is significantly lower than that for steel RC member with similar geometry.

The design of GFRP RC flexural member is usually governed by serviceability requirements and results in a GFRP flexural reinforcement beyond that needed to achieve the desired strength. In this case, the failure is governed by concrete crushing (compression-controlled failure). This results in a larger concrete compression block at failure and smaller, more evenly distributed, cracks compared with a tension-controlled member. Due to this behavior, the internal shear resistance mechanism of the member is improved. Therefore, using Eq. (1) may yield a very conservative estimate of the shear strength of the member.

A more rational approach could be achieved by accounting for the influence of the axial stiffness of the reinforcement,  $AE$ , on the behavior of the member. Following this approach,  $V_{c,f}$  can be expressed in terms of the ratio of the longitudinal FRP reinforcement  $\rho_f$  and steel reinforcement  $\rho_s$  as follows (ACI 440, 2000):

$$V_{c,f} = \frac{\rho_f E_f}{\rho_s E_s} V_c \quad (2)$$

For practical design purposes the value of  $\rho_s$  is taken as half the maximum reinforcement ratio allowed by ACI 318 or  $0.375\rho_b$ . Using this approach, the ACI Committee 440 draft document gives the shear strength equation as follows:

$$V_{c,f} = \frac{\rho_f E_f}{90 \beta_1 f'_c} V_c \quad (3)$$

Eq. (3) is more appropriate for beams, where the steel reinforcement is typically in the neighborhood of  $0.375\rho_b$ .

Based on the ACI 318 approach, the thickness of a RC slab is chosen so that deflections will not be a problem. The desired flexural capacity is achieved by back-calculating the required amount of steel reinforcement, which may be governed by the code-

specified minimum amount of reinforcement to control cracking. Occasionally, the thickness will be governed by shear or flexure. Following this approach, the ratio of steel reinforcement of slabs could be significantly lower than that for beams. Accordingly, using Eq. (3) that considers a steel reinforcement ratio of  $0.375\rho_b$  for beams to predict the shear strength of FRP RC slabs could be overly conservative and may unnecessarily result in a need for increased depth of the slab to meet the shear requirement.

The proposed ACI 440's design equation to determine the shear contribution of FRP stirrups  $V_f$  is identical to that used for steel stirrups, as follows:

$$V_f = \frac{A_{fv} f_{fv} d}{s} \quad (4)$$

The design strength of FRP stirrups  $f_{fv}$  is based on a strain of 0.002 (stress of  $0.002E_f$ ). This stress level must be equal to or lower than the tensile stress in the bend portion of the stirrup,  $f_{fb}$ , which rarely controls the design.

The 0.002 strain limit was imposed to control the crack width and therefore ensure a better aggregate interlock. Accounting for the axial stiffness of longitudinal reinforcement and imposing a strain limit on the transverse reinforcement penalizes the shear strength of a member twice for the same reason and ultimately results in an uneconomical use of the reinforcement. In addition, FRP bars do not corrode; therefore a strain limit of 0.002 could be relaxed.

Summing the shear contribution of the concrete and the stirrups gives the nominal shear, as follows:

$$V_n = V_{cf} + V_f \quad (5)$$

## 1.2 Objectives of the research program

The objective of this research program is to verify the shear design approach and limits proposed by ACI committee 440H. In this paper, the following will be addressed: 1) the contribution of  $V_{cf}$  and  $V_f$  to the shear strength of the member, 2) the influence of the axial stiffness  $AE$  of longitudinal reinforcement on  $V_c$ , 3) the strain limit for design of GFRP stirrups and 4) applicability of the proposed design approach to GFRP RC beams and slabs.

## 2 EXPERIMENTAL PROGRAM

In total, seven beams and six slabs were tested to

investigate the shear performance. Table 1 gives the dimensions and reinforcement for all specimens. Table 2 gives the properties of the constituent material. All specimens were designed to fail in shear. All beams had a cross-section of 178 mm (width) by 330 mm (height) and were 2.4 m. Although the test span envisioned for this test was 1.5 m, the beams were cast with 2.4 m length to ensure that sufficient development length is provided for the longitudinal reinforcement. The depth to the centroid of the longitudinal reinforcement varied depending on their layout. All the beams were reinforced with longitudinal GFRP bars. Four beams (BM1, BM2, BM5 and BM6) were reinforced with GFRP stirrups (see Table 1). The stirrups were closed stirrups with 90 deg bents, were made of  $\phi 9.5$  deformed GFRP, and had a bent radius of 19 mm, as shown in Figure 1. All the stirrups for these beams were pre-bend to specification by the FRP manufacturer. Slabs SB 2, SB4 and SB5 had a cross-section of 460 mm (width) by 100 mm (height) while slabs SG1, SG2, and SG3 had a cross-section of 460 mm (width) by 150 mm (height). All the slabs were 2.7 m and were tested with a span of 2.1 m. The effective depth for test specimens depends on the size and layout of the reinforcement.

### 2.1.1 Test Setup and Instrumentation

All beam specimens were tested as simply supported members subjected to a three-point load as illustrated in Figure 2. The first beam was tested with a span of six feet. The rest of the beams were tested with a span of 1.5 m. All slab specimens were tested as simply supported beams with a span of 2.1 m and subjected to a four-point load, as shown in Figure 3. The distance between the two point loads was 0.6 m, as illustrated in Figure 3.

Linear variable differential transformers (LVDTs) were used to measure the vertical displacement at mid-span and quarter-span of each specimen. Strain gages were attached to GFRP and steel longitudinal bars at mid-span and quarter-points. In the beams, at least two stirrups were instrumented with strain gages. The strain gages were attached on vertical legs, close to the bent, and at mid-height of the vertical legs. A 440-kN (beams) or a 270-kN (slabs) load cell was used to measure the applied load.

### 2.2 Test Procedure

The data acquired for each test included

measurements of applied load, longitudinal and shear reinforcement strains, deflection, and crack widths.

Table 1. Reinforcement type and amount.

Beam	Type	Longitudinal			Transverse		
		$A_f$ (mm <sup>2</sup> )	d (mm)	$\rho_f/\rho_b$	Type	$A_v$ (mm <sup>2</sup> )	Spacing (mm)
BM1	GFRP	1142	279	6.59	GFRP	142	152
BM2	GFRP	1142	279	6.59	GFRP	142	203
BM5	GFRP	1142	279	6.30	GFRP	142	152
BM6	GFRP	593	287	3.28	GFRP	142	203
BM7	GFRP	1142	279	5.76			
BM8	GFRP	393	287	1.96			
BM9	GFRP	684	287	3.37			
SB2	GFRP	213	76	2.12			
SB4	GFRP	387	76	3.54			
SB5	GFRP	516	76	4.71			
SG1	GFRP	400	127	1.98			
SG2	GFRP	568	127	2.67			
SG3	GFRP	851	127	3.83			

Table 2. Material properties.

Beam	$f'_c$ (MPa)	Longitudinal			Transverse		
		Type	$f_{fu}$ (MPa)	$E_f$ (GPa)	Type	$f_{fu}$ (MPa)	$E_f$ (GPa)
BM1	2.41	GFRP	717	40.0	GFRP	717	40.0
BM2	2.41	GFRP	717	40.0	GFRP	717	40.0
BM5	2.52	GFRP	717	40.0	GFRP	717	40.0
BM6	2.52	GFRP	717	40.0	GFRP	717	40.0
BM7	2.41	GFRP	717	40.0			
BM8	2.41	GFRP	717	40.0			
BM9	2.41	GFRP	717	40.0			
SB2	2.55	GFRP	834	41.4			
SB4	2.55	GFRP	800	42.1			
SB5	2.55	GFRP	800	42.1			
SG1	2.55	GFRP	655	40.0			
SG2	2.55	GFRP	620	40.0			
SG3	2.55	GFRP	620	40.0			



Figure 1: GFRP stirrups.



Figure 2: Beam test setup.



Figure 3: Slab test setup.

Each test specimen was tested under quasi-static load that was applied in several cycles. In each

cycle, the load was slowly increased until the target load was achieved. At this stage, the crack widths were measured. This process was continued until failure was achieved.

### 3 EXPERIMENTAL RESULTS

#### 3.1 Beams

##### 3.1.1 Beams with shear reinforcement

For beams BM1, BM3, BM4, and BM5, failure was a combination of flexure and shear. At approximately 53 to 71 kN, flexural cracks were observed. As the load was increased, some of the cracks started to extend at 45 degree to form shear cracks. At maximum load, concrete crushing at the top was observed, indicating flexural failure. This was immediately followed by a sudden shear failure due to rupture of at least one of the GFRP stirrups crossing a diagonal crack. For all the cases, when the concrete cover was removed, rupture of the GFRP stirrup was observed at the bent of the stirrup, as shown in Figure 4. However, although in a flexural mode, the failure load for these beams was higher than that predicted based on the theoretical shear capacity (see Table 3).

For beam BM2, the first flexural crack was observed at approximately 62 kN. The crack on the left side of the beam started to extend diagonally to form a shear crack. This was followed by a number of smaller flexural and shear cracks. Failure of beam BM2 occurred at approximately 258 kN and was initiated by rupture of one of GFRP stirrup crossing the first diagonal crack, as shown in Figure 5. Beam BM6 failed in flexural mode at approximately 289 kN. No rupture of GFRP stirrups was observed when the concrete cover was removed.

Table 3 presents comparison of the theoretical and experimental results for the beams. Three theoretical values for shear failure were calculated,  $P_{0.002}$ ,  $P_{0.004}$  and  $P_{bent}$  based on a GFRP strain limit of 0.002, 0.004, and the strength of the bent portion of the stirrups,  $f_{f,b}$ , respectively. The concrete contribution  $V_{c,f}$  was calculated using ACI 440's proposed equation, Eq. (3). The theoretical load capacities based on these three limits were calculated as follows:

$$P_{0.002} = 2(V_{c,f} + V_{f0.002}) \quad (6)$$

$$P_{0.004} = 2(V_{c,f} + V_{f0.004}) \quad (7)$$

$$P_{bent} = 2(V_{c,f} + V_{fbent}) \quad (8)$$

Failure loads based on the flexural capacity of each beam  $P_{flex}$  were also calculated. In Table 3, it can be seen that the experimental loads  $P_{exp}$  exceeded those based on a 0.002 strain limit  $P_{0.002}$  for all the specimens. The average of  $P_{exp}/P_{0.002}$  was 1.97, indicating that the design approach based on this strain limit is overly conservative and that it may underestimate the shear strength by approximately 50 percent. For all the beam specimens, the experimental results  $P_{exp}$  were also larger than those based on 0.004 strain limit  $P_{0.004}$ , and the average  $P_{exp}/P_{0.004}$  was 1.34. These results indicate that the 0.004 strain limit is more appropriate and can better utilize the contribution of GFRP stirrups while maintaining a conservative design approach.

The experimental failure loads for beam BM2, the only beam to fail in shear, was smaller than that based on the strength of the bent of the GFRP stirrups  $P_{bent}$ . A ratio of  $P_{exp}/P_{bent}$  of 0.85 was calculated for beam BM2. This indicates that the stirrups did not achieve the theoretical bent strength at failure. It should be noted that, due to the failure mode of these specimens, the actual shear strength of the beams was not determined. The experimental loads at failure  $P_{exp}$  of beams BM1, BM5 and BM6 compared well with their flexural capacity  $P_{flex}$  calculated using the approach of ACI 440. The average of  $P_{exp}/P_{flex}$  for these beams was 1.02.



Figure 4: Rupture of GFRP stirrups



Figure 5: Shear failure (BM2).

Table 3: Comparison of theoretical and experimental results.

Beam	Analytical				Experimental	
	$P_{0.002}$ (kN)	$P_{0.004}$ (kN)	$P_{bent}$ (kN)	$P_{flexure}$ (kN)	Exp. (kN)	Failure
BM1	81.8	123.2	189.5	148.6	81.8	Flex/S
BM2	71.2	102.7	152.1	178.4	71.2	Shear
BM5	81.0	122.3	188.6	183.7	81.0	Flex/S
BM6	52.9	85.0	135.7	150.3	52.9	Flex/S

Figure 6 shows a breakdown of the measured internal shear resistance for beam BM2 that failed in shear mode. In this figure, experimental values of  $V_f$  were calculated using the measured strain of GFRP stirrups. The strain measurements were obtained from the strain gage located at the bent of the ruptured stirrups. As shown in this figure, prior to cracking, the internal shear resistance was provided by the solid beam section. Once the beam cracked, the shear stirrups started to pick up strain, indicating a shear resistance contribution by the stirrups. The shear resistance provided by the concrete  $V_{cf}$  after cracking was slightly lower than that of the solid section prior to cracking. However, as the load was increased, the  $V_{cf}$  also increased and the value of the internal shear resistance provided by concrete at failure was slightly larger than that of the solid section.

### 3.1.2 Beams without shear reinforcement

Beams BM7 through BM9 (no shear reinforcement) failed in shear, as given in Table 5. The test results of these beams show that the current design approach is very conservative. The average ratio of

experimental to theoretical failure load  $P_{exp}/P_{theo}$  was 3.27. Figure 7 show that increasing the amount of longitudinal reinforcement significantly increased the shear strength of the beams. Figure 8 shows the relation between  $V_{c,f,exp}/V_{440}$  ratio and the ratio of the GFRP reinforcement to the balanced ratio of reinforcement,  $\rho_f/\rho_{f,b}$ , calculated per ACI 440. In this figure, it can be seen that the relationship between the two ratios is non-linear and that as the ratio of  $\rho_f/\rho_{f,b}$  increased, the ratio of  $V_{c,f,exp}/V_{440}$  reduced.

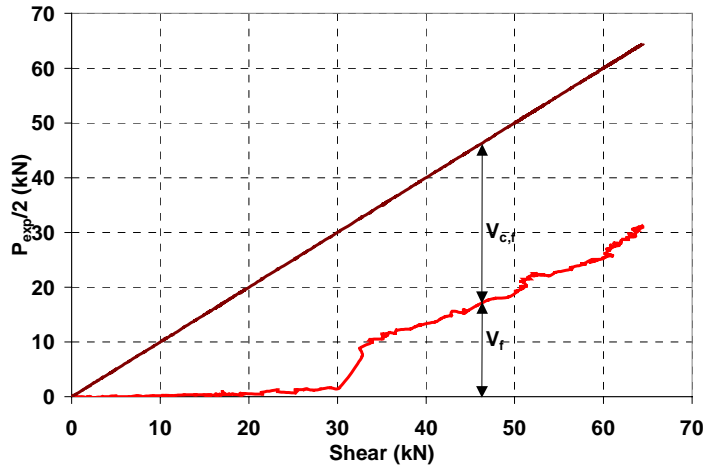


Figure 6: Components of internal shear resistance for (BM2).

Table 5: Comparison of Beam Results (w/o stirrups).

Beam	Theoretical		Experimental		$P_{exp}/P_{theo}$
	$P_{440}$ (kN)	$P_{flex.}$ (kN)	$P_{exp.}$ (kN)	Failure	
BM7	40.0	177.9	106.8	Shear	2.66
BM8	13.8	124.5	72.1	Shear	5.18
BM9	24.0	154.3	80.1	Shear	3.31

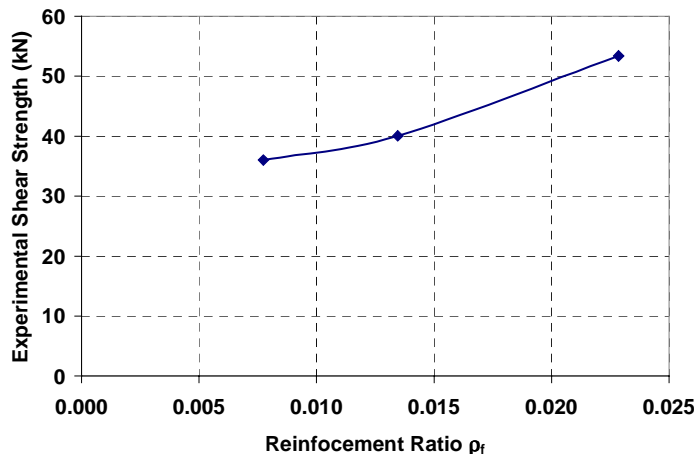


Figure 7: Comparison of results for beams w/o stirrups.

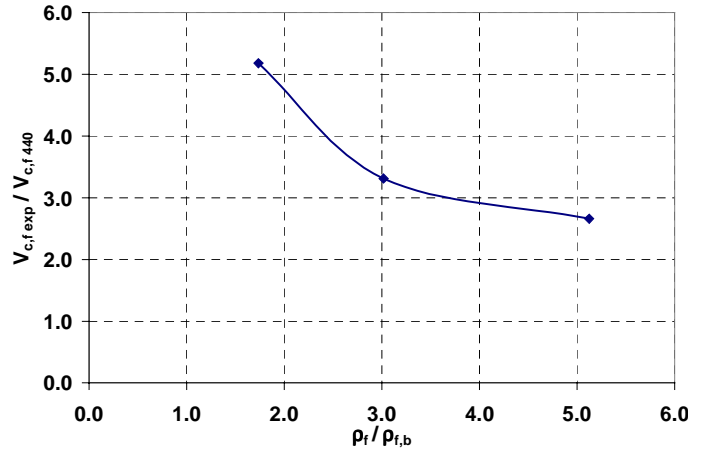


Figure 8: Comparison of results for beams w/o stirrups.

### 3.2 Slabs

Table 6 shows a comparison of the predicted and the experimental loads at failure of the slabs. All the slabs failed in flexure at a load higher that predicted based on shear failure per ACI 440. In Table 6, the theoretical failure load values  $P_{440}$  were based on the design approach of ACI 440, Eq. (3). The values of  $P_{440}/P_{theo}$  for these test varied from 1.58 to 3.21 with an average of 2.24, indicating that the proposed design approach for GFRP RC slabs is very conservative.

Table 6: Comparison of Slab Results (kips).

Beam	Theoretical		$P_{exp}$ (kN)	Failure	$P_{exp}/P_{theo}$
	$P_{theo}$ (kN)	$P_{flex.}$ (kN)			
SB2	7.6	15.5	17.7	Flexure	2.34
SB4	14.0	19.8	21.5	Flexure	1.54
SB5	18.6	22.1	29.4	Flexure	1.58
SG1	14.1	43.1	45.4	Flexure	3.21
SG2	20.1	49.6	53.8	Flexure	2.68
SG3	30.1	57.8	63.6	Flexure	2.11

## 4 SUMMARY AND CONCLUSIONS

The shear performance of seven beams and six slabs reinforced with different amounts of longitudinal and transverse GFRP reinforcement was investigated. The objective was to examine shear design approach of ACI 440 and to produce additional data to examine the shear performance of RC members reinforced for shear and/or flexure using GFRP bars.

GFRP bars are the most common type of FRP reinforcement and have been therefore considered for this investigation. All specimens were designed to fail in shear.

Based on the test results presented in this paper for the beams and slabs with the given geometry and material properties, the following conclusions can be drawn:

- Except for beam BM2, all the beams with shear reinforcement failed in a flexure-shear mode. Their actual shear strength was not determined.
- The flexure-shear failure mode started as flexural failure that was followed by shear failure due to GFRP stirrup rupture that was caused by the loss of the internal shear resistance provided by the compression concrete, which led to failure of the stirrup due to overloading.
- Beam B2 failed in shear mode by rupture of a GFRP stirrup at the bent. The measured stress at failure was below the strength of the bent,  $f_{fb}$ .
- Independent of the failure mode, all test specimens failed at a load significantly higher than that predicted using the approach by ACI 440.
- The strain limit of 0.002 for the design of GFRP stirrups is very conservative and could be relaxed to 0.004 while maintaining a reasonably conservative design.
- The design approach proposed by ACI 440 for the shear strength  $V_{c,f}$  of GFRP RC flexural members in which the failure mode is governed by concrete crushing (compression-controlled) is overly conservative.
- The experimental shear strength of the beams with no stirrups  $V_{c,f}$  was proportional to the amount of longitudinal GFRP reinforcement. As the amount of GFRP reinforcement increased, the experimental shear strength increased.
- Due to the flexural failure mode, actual shear strength of the slabs could not be determined. However, it can conservatively be said that for over-reinforced slabs with  $\rho_f/\rho_{fb}$  larger than 2, the actual shear strength of the slab can be at least 1.5 times higher than that predicted using the ACI 440 design approach.
- The flexural capacity of all test specimens compared well with the predicted values using the approach of ACI 440.

## 5 ACKNOWLEDGMENTS

This research program is being funded by the Industry/University National Science Foundation (NSF) research center at the University of Missouri-Rolla.

## REFERENCES

- ACI Committee 318. 1995. Building Code Requirements for Structural Concrete (ACI 318-95) and Commentary (ACI 318R-95). American Concrete Institute, Farmington Hills, Michigan, USA. 369 pp.
- ACI Committee 440. 2000. Guide for the Design and Construction of Concrete Reinforced with FRP Bars. Final Draft (in print).
- ACI-ASCE Committee 426. 1978. Suggested Revisions to Shear Provisions for Building Codes. American Concrete Institute, Farmington Hills, Michigan, USA. 88 PP.
- Nagasaka, T., Fukuyama, H., & Tanigaki, M. 1993. Shear Performance of Concrete Beams Reinforced with FRP Stirrups. *Fiber-Reinforced-Plastic Reinforcement for Concrete Structures*. SP-138. American Concrete Institute. Farmington Hills, Michigan, USA. 789-811.
- Michaluk, C.R., Rizkalla, S., Tadros, G., & Benmokrane, B. 1998. Flexural Behavior of One-Way Concrete Slabs Reinforced by Fiber Reinforced Plastic Reinforcement. *Structural Journal* 95(3): 353-364.
- Sonobe, Y., Fukuyama, H., Okamoto, T., Kani, N., Kimura, K., Kobayashi, K., Masuda, Y., Matsuzaki, Y., Mochizuki, S., Nagasaka, T., Shimizu, A., Tanano, H., Tanigaki, M., and Teshigawara, M. 1997. Design Guidelines of FRP Reinforced Concrete Building Structures. *Journal of Composites for Construction* 1(3): 90-113.